A restricted dimer model on a 2-dimensional random causal triangulation

J. Ambjørn [a,d], B. Durhuus [b], and J.F. Wheater [c]

[a] The Niels Bohr Institute, Copenhagen University
Blegdamsvej 17, DK-2100 Copenhagen Ø, Denmark.
email: ambjorn@nbi.dk

[b] Department of Mathematical Sciences, Copenhagen University,
Universitetsparken 5, DK-2100 Copenhagen Ø, Denmark.
email: durhuus@math.ku.dk

[c] Rudolf Peierls Centre for Theoretical Physics, Oxford University,
1 Keble Road, Oxford OX1 3NP, UK.
email: j.wheater@physics.ox.ac.uk

[d] IMAPP, Radboud University,
Heyendaalseweg 135, 6525 AJ, Nijmegen, The Netherlands

Abstract

We introduce a restricted hard dimer model on a random causal triangulation that is exactly solvable and generalizes a model recently proposed by Atkin and Zohren [16]. We show that the latter model exhibits unusual behaviour at its multicritical point; in particular, its Hausdorff dimension equals 3 and not 3/2 as would be expected from general scaling arguments. When viewed as a special case of the generalized model introduced here we show that this behaviour is not generic and therefore is not likely to represent the true behaviour of the full dimer model on a random causal triangulation.

PACS: 04.60.Ds, 04.60.Kz, 04.06.Nc, 04.62.+v.
Keywords: quantum gravity, low dimensional models, lattice models.

1 Introduction

The study of statistical theories of fluctuating geometries is important for a number of reasons. Regularized via appropriate lattices, so-called Dynamical Triangulations (DT)[1]), they may serve as rigorous definitions of the path integral of bosonic string theories [2], or quantum gravity [3]. The DT formalism has been immensely successful in the study of two-dimensional quantum gravity coupled to conformal field theories with central change $c \leq 1$, also known as non-critical string theory or Liouville quantum gravity, but it has been less successful serving as a regularization of a putative higher dimensional quantum gravity theory [4]. In an attempt to improve the situation a modified lattice regularization, called the Causal Dynamical Triangulation (CDT), was proposed in which a foliation structure is imposed on the lattices representing space-time (which we here will assume has Eucliean signature) [5, 6]). Such a foliation structure is also imposed in the so-called Hořava-Lifshitz gravity theory [7]. Some interesting results related to higher dimensional quantum gravity have been obtained using the CDT regularization (see [8] for a review). Here we will discuss the two-dimensional CDT theory, which in principle should be simpler than the corresponding two-dimensional DT theory. Indeed, the scaling limit of CDT not coupled to matter is simple [5, 9], and it can be shown to correspond to two-dimensional Hořava-Lifshitz quantum gravity [10]. However, in contrast to the case of two-dimensional DT, it has been difficult to obtain solvable models of two-dimensional CDT coupled to field theories. The only analytically solvable example of an explicit field theory system coupled to gravity is provided by CDT coupled to gauge fields [11], but two-dimensional gauge field theories are mainly topological, so the systems obtained are very simple from a matter perspective.

Computer simulations indicate that for unitary conformal field theories with central charge $c \leq 1$ the coupling between matter and geometry is weak [12, 13] with the critical exponents of both the matter theories and the geometry apparently unchanged. This is in sharp contrast to the DT situation, where both matter and geometric exponents are shifted relative to the matter exponents in flat spacetime and the geometric exponents in 2d Liouville gravity without matter. According to the computer simulations the situation changes when the central charge c of the matter fields coupled to CDT is larger than one indicating that the coupling to geometry then becomes strong [14, 15].

Thus it was interesting and surprising when it was shown that restricted dimer systems coupled to CDT could be solved analytically and seemingly led to a change of the critical exponents of the geometry [16, 17]. It is well known that the hard dimer model on a regular two-dimensional lattice exhibits critical behaviour

[1]There are other ways to provide lattice regularizations of bosonic string theory, e.g. using hypercubic lattices [1].

for a certain negative value of the fugacity, and that this critical system can be associated with a (2,5) minimal non-unitary field theory having central charge $c = -22/5$. In fact, it can be identified via the high temperature expansion of the Ising model in an imaginary magnetic field with the Lee-Yang edge singularity. In [22] it was shown that a similar identification of a critical hard dimer model with the Lee-Yang edge singularity can be made in the DT case and the critical exponents can be calculated. One finds again a non-trivial interaction between geometry and matter, but it is weaker than the interaction between the unitary models and geometry. This is in accordance with the expectation that when $c \to -\infty$ matter and gravity decouple. Thus the change in critical geometric properties found in [16, 17] when coupling the CDT model to some classes of restricted dimers is puzzling: for unitary models with $0 < c \leq 1$ we have a weak coupling and no change in critical geometric properties of the geometry, as mentioned above. Naively we would expect the dimer systems at criticality to correspond to non-unitary field theories with central charge $c < 0$ and thus an even weaker coupling, by analogy to the DT systems. This has motivated us to take a closer look at the model proposed in [16] (hereafter called the AZ model). As we will report below the model is more subtle than anticipated in [16].

The rest of this article is organized as follows. In Sec. 2 we define a generalized AZ model and discuss its basic properties. In Sec. 3 we consider the two-point function in the AZ model in a grand canonical setting and we use it to calculate the global Hausdorff dimension d_H. Sec. 4 addresses the calculation of the so-called local Hausdorff dimension d_h in a microcanonical setting. We find somewhat surprisingly that $d_h = d_H = 3$. In Sec. 5 we show that this result is very special and probably not representative for an unrestricted hard dimer model coupled to CDT. We do this by analyzing in some detail the extended AZ model which allows more general dimer configurations while remaining solvable. The AZ model corresponds to one particular point in the phase boundary of this generalized model and we show that it is the only point at which the Hausdorff dimensions assume the value 3, while the values at other points are either $d_H = 3/2$ and $d_h = 1$ or $d_H = d_h = 2$. Sec. 6 contains a discussion of the results and arguments in favour of viewing $d_H = 3/2$ as correct also for the unrestricted dimer model coupled to CDT, i.e. for a $c = -22/5$ conformal field theory coupled to 2d Hořava-Lifshitz gravity. Finally, the Appendix discusses the general conditions responsible for the special features of the AZ model.

2 A restricted dimer model, basic properties

We consider an extension of the dimer system on random causal triangulations first introduced in [16]. A finite causal triangulation T of the planar disc $\mathcal{D}$, is

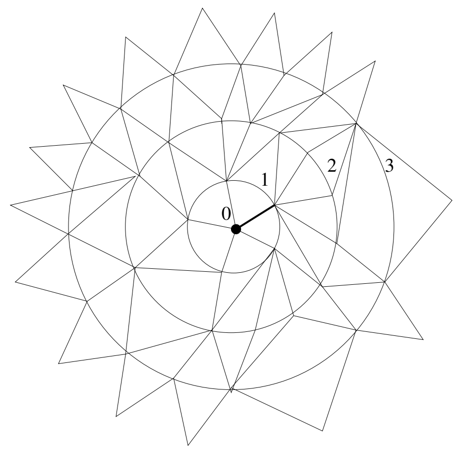

Figure 1: A causal triangulation.

constructed as shown in Fig 1. T is the union of a central disc Σ_0 having *central vertex* v_0 and boundary circle S_1, and a sequence of annuli (or time slices) Σ_k, $k > 1$, such that Σ_k is bounded by circles S_{k-1} and S_k. For $k \geq 1$, Σ_k is triangulated by a circular array of triangles each of which contains either one vertex in S_{k-1} and two vertices in S_k, called a *backward directed triangle*, or two vertices in S_{k-1} and one vertex in S_k, called a *forward directed triangle*. Σ_0 is triangulated by a sequence of triangles sharing the central vertex, which we define to be backward directed. Edges contained in one S_k are called *horizontal edges*. By convention we adjoin a forward directed triangle to each of the outermost horizontal edges (see Fig 1) so that all horizontal edges are shared by a forward and a backward directed triangle. We assume in the following that the edges/vertices in S_k and triangles in Σ_k are ordered clockwise, and it is convenient to assume also that one of the edges emanating from the central vertex is marked.

Given a vertex $v \neq v_0$ in S_k we denote by $e(v)$ the horizontal edge in T emanating in positive clockwise direction from v, by $\Delta(v)$ the forward directed triangle containing $e(v)$ in its boundary, and by $f(v)$ the non-horizontal edge in $\Delta(v)$ emanating from v, see Fig 2. Moreover, the *forward degree* $\sigma_f(v)$ and the *backward degree* $\sigma_b(v)$ of v are defined as the number of neighbours of v in S_{k+1} and S_{k-1}, respectively. Note that $\sigma_f(v), \sigma_b(v) \geq 1$ and that $\sigma_f(v) = 1$ if and only if $e(v)$ separates two forward directed triangles.

Given a causal triangulation T, let $\tilde{T}$ denote its dual graph. A *restricted dimer configuration* D on $\tilde{T}$ is a set of edges in $\tilde{T}$ fulfilling

a) no pair of edges in D share a vertex in $\tilde{T}$;

b) edges in $\tilde{T}$ dual to edges in T that separate two backward directed triangles are not admissible in D;

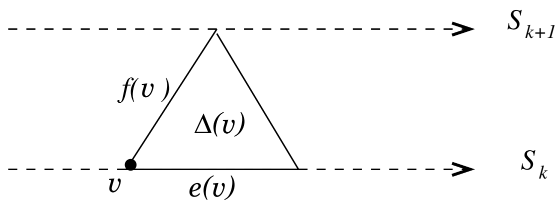

Figure 2: Labelling the edges of a forward directed triangle. The arrows indicate the clockwise direction on the time slices.

c) if $v \in S_k$, $k > 0$, is a vertex with $\sigma_f(v) = 1$, then $f(v)$ is not dual to a dimer if either $\sigma_b(v) > 1$ or if $\sigma_b(v) = 1$ and the successor w to v in S_k has $\sigma_b(w) > 1$.

Here, condition a) is the standard requirement specifying a dimer configuration, while b) and c) represent further technical conditions allowing an exact solution by utilizing a mapping onto labelled trees as demonstrated below.

The possible dimer types are illustrated in Fig 3. Dimers dual to horizontal edges we call type 1, while those shared by a forward and a backward directed triangle in the same time slice we call types 2 and 2' respectively depending on whether or not the backward triangle precedes the forward triangle w.r.t. clockwise ordering. Type 3 dimers are those dual to edges shared by two forward directed triangles. Finally we denote by D_i the set of edges of type i in D so that $D = D_1 \cup D_2 \cup D_{2'} \cup D_3$.

The grand canonical ensemble we are interested in consists of elements (T, D) specified by a causal triangulation T and an admissible dimer configuration D on $\tilde{T}$. With the three types of dimers we associate fugacities $\xi_1, \xi_2, \xi_{2'}, \xi_3$ and define the partition function

$$Z(\xi_1, \xi_2, \xi_{2'}, \xi_3; g) = \sum_{(T,D)} g^{|T|/2} \xi_1^{|D_1|} \xi_2^{|D_2|} \xi_{2'}^{|D_{2'}|} \xi_3^{|D_3|} , \tag{1}$$

where $|A|$ denotes the number of elements in a set A. It is easy to show that $Z(\xi_1, \xi_2, \xi_{2'}, \xi_3; g)$ is well defined for any fixed values of $\xi_1, \xi_2, \xi_{2'}, \xi_3$ provided that $|g|$ is sufficiently small.

It is straightforward to see [16] that Z is a function of $\xi_2 + \xi_{2'}$ for fixed g and ξ_1, ξ_3. Therefore, we shall henceforth set $\xi_{2'} = 0$, i.e. we further restrict dimer configurations such that $D_{2'} = \emptyset$, and drop ξ_2' from the notation and write $\vec{\xi} = (\xi_1, \xi_2, \xi_3)$. Note that for $\xi_2 = \xi_3 = 0$ we have $Z(\xi_1, 0, 0; g) = Z(0, 0, 0; g(1 + \xi_1))$, since the number of triangles in a causal triangulation equals twice the number of horizontal edges and because horizontal dimers are mutually independent in the absence of non-horizontal dimers.

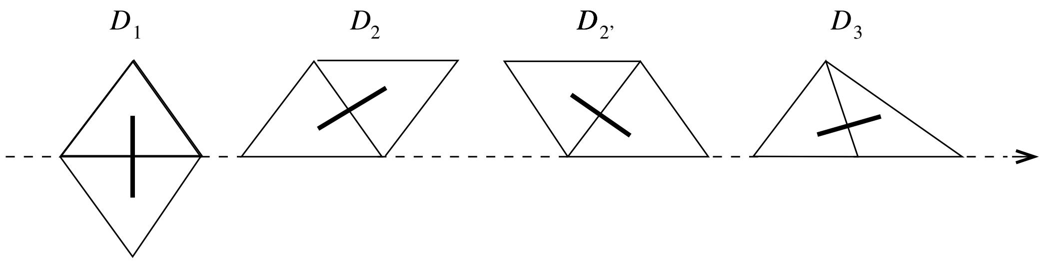

Figure 3: Dimer Types. The arrow indicates the clockwise direction on a time slice.

In order to determine the analyticity properties of Z we shall, as mentioned, exploit a correspondence between admissible pairs (T, D) and certain labelled trees which we now explain by slightly generalising a construction given in [16]. From a causal triangulation T one obtains a planar rooted tree $\tau = \beta(T)$ in the following way:

i) delete all boundary edges (those belonging to the outmost forward directed triangles);

ii) delete all horizontal edges $e(v)$ and all non-horizontal edges of the form $f(v)$ for $v \in T$;

iii) attach a new root edge to v_0 such that the marked edge in T is the rightmost edge emanating from v_0 in $\beta(T)$.

It was shown in [18] that β yields a bijective correspondence between causal triangulations with $2n$ triangles and rooted planar trees with n+2 vertices and root of order 1. Note that the vertices of $\beta(T)$ different from the root are also vertices of T and that from now on when referring to a tree we will denote the vertex next to the root by v_0 and call it the *first vertex* of the tree. A dimer configuration D on $\tilde{T}$ induces the following labelling ℓ of the vertices of the tree $\tau = \beta(T)$:

1) if $e(v)$ is dual to a dimer in D, set $\ell(v) = 1$;

2) if $f(v)$ is dual to a dimer in D and $\sigma_f(v) > 1$, set $\ell(v) = 2$;

3) if $f(v)$ is dual to a dimer in D and $\sigma_f(v) = 1$, set $\ell(v) = 3$;

4) the root is unlabelled;

5) otherwise, set $\ell(v) = 0$.

The restrictions imposed on D are equivalent to the following constraints on ℓ:

a) if a leaf of $\beta(T)$ has label 3 then its preceding neighbour at same height has label 0 and its successor at same height has label 0 or 1;

b) if a vertex in $\beta(T)$ that is not a leaf has label 2, then its rightmost decendant does not have label 1;

c) a leaf of $\beta(T)$ that is the leftmost or the rightmost decendant of its predecessor does not have label 3.

Noting that all edges in T dual to dimers in D are deleted when constructing $\beta(T)$, it is straightforward to show that the correspondence between pairs (T, D) and pairs (τ, ℓ) with $\ell(v_0(\tau)) = 0$ is bijective. Note also that the number ℓ_i of vertices in $\beta(T)$ with label i equals $|D_i|$ for $i = 1, 2, 3$.

Consider now a labelled tree (τ, ℓ) as above and assume the vertex v_0 next to the root has order $s + 1$, i.e. τ has s branches $\tau_1, \ldots, \tau_s$ rooted at v_0. Since $\ell(v_0(\tau)) = 0$ the labellings of the τ_i induced by the labelling of τ are independent and the labelling of the first vertex is unrestricted. However, the labellings of the different branches rooted at the vertex $v_0(\tau_i)$ may, depending on its label, not be independent due to the constraints a) and b). Now define the partition function for trees whose first vertex has label i to be

$$W_i(\vec{\xi}; g) = \sum_{(\tau,\ell):\ell(v_0)=i} g^{|\tau|} \xi_1^{\ell_1} \xi_2^{\ell_2} \xi_3^{\ell_3}, \qquad i = 0, 1, 2, \tag{2}$$

where $|\tau|$ denotes the number of edges in τ. Then decomposing trees into the root edge and their branches rooted at v_0 shows that the W_i satisfy the equations

$$W_i = F_i(W_0, W_1, W_2; \vec{\xi}; g)\,, \tag{3}$$

where

$$\begin{aligned}
F_0 &= g\,(1 - g\xi_3 W_0) H \\
F_1 &= g\,\xi_1 (1 - g\xi_3 W_0) H \\
F_2 &= g\,\xi_2\,(W_0 + (1 - g\xi_3 W_0) W_2)\, H
\end{aligned}$$

with

$$H = \{1 - (1 + g\xi_3) W_0 - W_1 - (1 - g\xi_3 W_0) W_2\}^{-1}\,. \tag{4}$$

It follows from the discussion above that

$$Z(\vec{\xi}; g) = g^{-1} W_0(\vec{\xi}; g) - 1\,, \tag{5}$$

and that non-analytic behaviour of $Z(\vec{\xi}; g)$ as a function of g at a critical point $g_c(\vec{\xi})$, of the form

$$Z_c - Z(\vec{\xi}; g) \sim (g_c - g)^{\alpha}\,,$$

for some $0 < \alpha < 1$, occurs if and only if W_0 exhibits the same behaviour

$$W_{0c} - W_0(\vec{\xi}; g) \sim (g_c - g)^\alpha \,. \tag{6}$$

Here and in the following the notation $a \sim b$ is used to indicate that there exist constants $c_1, c_2 > 0$ such that $c_1\, a \le b \le c_2\, a$. By eliminating W_1, W_2 from (3) we obtain

$$(\xi_1 + g\xi_3)\xi_2 W_0^3 - (1 + \xi_1 + \xi_2 + g\xi_3 + g^2\xi_2\xi_3)W_0^2 + (1 + g\xi_2 + g^2\xi_3)W_0 - g = 0 \tag{7}$$

which, for fixed $\vec{\xi}$, determines W_0 as the unique root vanishing and analytic at $g = 0$. For $\xi_1, \xi_2, \xi_3 \ge 0$ the Taylor expansion of W_0 obtained from (2) has positive coefficients and hence its radius of convergence $g_c > 0$ is a singularity of W_0. This is a property of W_0 that persists, as we shall see, in a larger range S of couplings ξ_1, ξ_2, ξ_3 that are not necessarily positive. For generic $\vec{\xi}$ in this range, W_{0c} is a double root of (7) at $g = g_c$ and g_c is a square root branch point of W_0 as a function of g. If $\vec{\xi} \in S$ is such that W_{0c} is a triple root of (7) at $g = g_c$, i.e. $\alpha = 1/3$ in (6), then $(\vec{\xi}; g_c)$ is a multicritical point which we denote by $(\vec{\xi}_c; g_c)$.

The condition that g_c be a double root is obtained by differentiating (7) w.r.t W_0, so that the critical coupling g_c and the corresponding value W_{0c} of W_0 satisfy

$$3(\xi_1 + g_c\xi_3)\xi_2(W_{0c})^2 - 2(1 + \xi_1 + \xi_2 + g_c\xi_3 + g^2\xi_2\xi_3)W_{0c} + (1 + g_c\xi_2 + g_c^2\xi_3) = 0. \tag{8}$$

Using this in (7) yields

$$(1 + \xi_1 + \xi_2 + g_c\xi_3 + g_c^2\xi_2\xi_3)(W_{0c})^2 - 2(1 + g_c\xi_2 + g_c^2\xi_3)W_{0c} + 3g_c = 0. \tag{9}$$

and g_c and W_{0c} are determined as functions of $\vec{\xi}$ by (8) and (9).

Multicritical points additionally satisfy

$$3(\xi_{1c} + g_c\xi_{3c})\xi_{2c}W_{0c} - (1 + \xi_{1c} + \xi_{2c} + g_c\xi_{3c} + g_c^2\xi_{2c}\xi_{3c}) = 0\,. \tag{10}$$

The existence of such multicritical points can be established by e.g. setting $\xi_1 = \xi$, $\xi_2 = \kappa\xi$ and $\xi_3 = 0$, where $\kappa > 0$. The value $\kappa = 2$ corresponds to the AZ model considered in [16]. However the results are universal for $\kappa > 0$ and we will denote all these models as AZ models, and explicitly perform the calculations for $\kappa = 1$ (except in footnote 2 where we discuss the situation of an arbitrary real value of κ). For $\kappa = 1$ we use (8), (9) and (10) to obtain the equation

$$\xi_c^3 + 24\xi_c^2 + 3\xi_c - 1 = 0 \tag{11}$$

for the critical value of ξ. This polynomial has one positive root and two negative roots and a closer analysis shows that the largest negative root $\xi_c \approx -0.278$ corresponds to a multicritical point $(\xi_c, \xi_c, 0; g_c)$, while g_c is a square root singularity of W_0 for $\xi > \xi_c$ (for a discussion of the situation for a general value of κ see footnote 2).

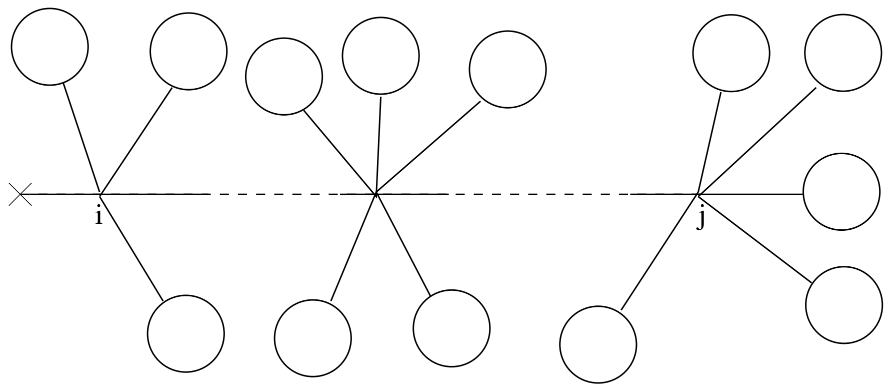

Figure 4: Graphical illustration of $\mathbb{G}(\xi, g; r)_{ij}$.

3 The two-point function for $\xi_1 = \xi_2 = \xi, \xi_3 = 0$

We now consider the fractal behaviour of triangulations and the corresponding labelled trees close to the critical point for the AZ model. The Hausdorff dimension in the grand canonical ensemble is determined by the decay rate of the two point function [19].

Concentrating first on trees define a marked labelled tree to be a triple (v, τ, ℓ) where (τ, ℓ) is a labelled tree as above and v is a vertex in τ different from the root and the first vertex v_0. By $d(v)$ we denote the graph distance from the root to v. The two-point function $\mathbb{G}(\xi, g; r)$ is defined by

$$(\mathbb{G}(\xi, g; r))_{ij} = W_j^{-1} \sum_{(v,\tau,\ell):\ell(v_0)=i,\ell(v)=j,d(v)=r+1} g^{|\tau|} \xi^{\ell_1+\ell_2},$$

for $i, j \in \{0, 1, 2\}$ and $r \geq 1$. A schematic illustration of the two-point function is shown in Fig. 4, from which it follows by standard arguments and considerations similar to those leading to (3) that

$$\mathbb{G}(\xi, g; r) = \mathbb{T}(\xi, g)^r, \tag{12}$$

where

$$(\mathbb{T}(\xi, g))_{ij} = \frac{\partial F_i}{\partial W_j} \tag{13}$$

which after some simplification gives

$$\mathbb{T}(\xi, g) = g^{-1} W_0^2 \begin{pmatrix} 1 & 1 & 1 \\ \xi & \xi & \xi \\ \xi(1 - \xi W_0) & \xi W_0 (1 - \xi W_0)^{-1} & \xi(1 - \xi W_0) \end{pmatrix}. \tag{14}$$

Clearly, the matrix $\mathbb{T}$ has one eigenvalue $\lambda_3 = 0$. The two other eigenvalues, λ_1 and λ_2, are solutions of the characteristic equation

$$\lambda^2 - \Big(-1 + (1+\xi g)\frac{W_0}{g}\Big)\, \lambda + \frac{\xi^2 W_0^3}{g} = 0. \tag{15}$$

which we rewrite as

$$\Big(\lambda - 1\Big)\Big(\lambda - \frac{\xi^2 W_0^3}{g}\Big) + \lambda(1-\xi W_0)\,\frac{W_0}{g}\,\frac{\partial g}{\partial W_0} = 0. \tag{16}$$

On the critical line $(W_{0c}(\xi), g_c(\xi))$, $\xi \geq \xi_c$, the last term vanishes and

$$\lambda_1 = 1, \quad \lambda_2 = \frac{\xi^2 W_{0c}(\xi)^3}{g_c(\xi)} \quad \text{for } \ \xi \geq \xi_c. \tag{17}$$

In particular, for $\xi = 0$ we have $W_{0c} = 1/2$, $g_c = 1/4$ and $\lambda_2 = 0$. As ξ decreases from zero to $\xi_c \approx -0.278$ we find that λ_2 increases monotonically to $\lambda_{2c} = 1$, where the value 1 is a simple consequence of (7) and (10).

For fixed $\xi > \xi_c$ the two eigenvalues are real for $\Delta g = g - g_c$ small enough and the dominant eigenvalue is λ_1 approaching 1 as $g \to g_c$. Hence, we get in this case

$$\mathbb{G}(\xi, g; r) = e^{-m(g)r + o(r)}$$

as $r \to \infty$, where

$$m(g) \sim \Delta\lambda_1 = 1 - \lambda_1\,.$$

At the critical line for $\xi > \xi_c$ we have $g'(W_0) = 0$ and $g''(W_0) \neq 0$, i.e. $\alpha = 1/2$ in eq. (6). Thus we obtain from (16)

$$\Delta\lambda_1 \sim \frac{\partial g}{\partial W_0} \sim |\Delta g|^{\frac{1}{2}}. \tag{18}$$

Hence, the two-point functions decay exponentially with rate

$$m(g) \sim |\Delta g|^{\frac{1}{2}}\,.$$

This shows that for the labelled trees with $\xi > \xi_c$ the *global Hausdorff dimension*, defined as the inverse of the critical exponent of $m(g)$ (see e.g. [19]), is $d_H = 2$.

At the multicritical point (ξ_c, g_c), on the other hand, we have $g'(W_0) = g''(W_0) = 0$ and $\alpha = 1/3$ in (6). Using this and (10) gives

$$(1 - \xi_c W_0)\frac{\partial g}{\partial W_0} = 3\xi_c^2 (\Delta W_0)^2 + \xi_c \Delta g\,, \tag{19}$$

where $\Delta W_0 = W_0 - W_{0c}$. Inserting this expression into (16) and setting $\Delta\lambda = 1-\lambda$ now gives[2]

$$(\Delta\lambda)^2 + \frac{3}{W_{0c}}\,\Delta\lambda\,\Delta W_0 + \frac{3}{(W_{0c})^2}\,(\Delta W_0)^2 = O(\Delta W_0^3), \tag{20}$$

and hence

$$\Delta\lambda = \frac{3}{2W_{0c}}|\Delta W_0|(1 \pm i/\sqrt{3}) + O(\Delta W_0^2). \tag{21}$$

In particular, $\lambda_1 = \overline{\lambda}_2$ is complex for $g < g_c$ in this case and we conclude that $\mathbb{G}(\xi, g; r)$ decays exponentially (dressed with oscillating factors) with decay rate

$$m(g) \sim \mathrm{Re}\,\Delta\lambda \sim |\Delta W_0| \sim |\Delta g|^{\frac{1}{3}}\,.$$

This yields the value $d_H = 3$ for the global Hausdorff dimension at $\xi = \xi_c$.

Returning to the dimer model on causal dynamical triangulations the two-point function $G(\xi, g; r)$ is defined in the same manner as for trees by marking a vertex v at distance $d(r)$ from the central vertex of the triangulation T and setting

$$G(\xi, g; r) = \sum_{(v,T,D):d(v)=r} g^{|T|/2}\xi^{|D_1|+|D_2|}\,.$$

Using the mapping β between the dimer model and the labelled tree model we obtain

$$G(\xi, g; r) = g^{-1}\sum_j \mathbb{G}_{0j}(\xi, g; r)W_j(g)\,.$$

In particular, $G(\xi, g; r)$ has the same exponential decay rate as the two-point functions $\mathbb{G}(\xi, g; r)_{ij}$, and hence the global Hausdorff dimension of the dimer model coincides with that of the labelled tree model, i.e. $d_H = 2$ for $\xi > \xi_c$ and $d_H = 3$ for $\xi = \xi_c$.

---

[2] One can repeat the calculations leading to (20) for the general assignment $\xi_1 = \xi$, $\xi_2 = \kappa\xi$, $\xi_3 = 0$, $\kappa > 0$, and find that (20) is independent of κ. However the values of W_{0c}, g_c and ξ_c depend on κ. What is important is the existence of a multicritical point ξ_c. For $\kappa = 1$ this was ensured by eq. (11). The equation for a general κ is

$$-b^3\xi_c^3 + 3(9-b^2)\xi_c^2 - 3b\xi_c - 1 = 0, \quad \kappa = b + 2.$$

For $\kappa > 0$ the largest real negative root corresponds to the multicritical point, precisely as in (11). Interestingly, for the original AZ value $b = 0$ the equation simplifies to a trivial second order equation (it is the point where the equation changes from having two negative and one positive solution to one negative and two positive solutions, the third root moving to $-\infty$ for $b \to 0^-$ and to ∞ for $b \to 0^+$). However, this has no consequences for the discussion of multicriticality. For $\kappa < 0$ there is no negative real solution.

4 The infinite size limit

In this section we consider an alternative notion of Hausdorff dimension for the labelled tree model by considering only critical trees, i.e. we shall evaluate the infinite size limit first and express the Hausdorff dimension in terms of volume growth on infinite trees. In order to make this precise, let us introduce the finite size partition functions $W_{iN}(\vec{\xi})$ by restricting the sum in (2) to trees τ of fixed size N, so that

$$W_i(\vec{\xi};g) = \sum_N g^N W_{iN}(\vec{\xi})\,.$$

The distributions μ_{iN} of labelled trees of fixed size N are obtained by normalizing the weights defining W_{iN}, i.e.

$$\mu_{iN}(\tau,\ell) = \frac{1}{W_{iN}(\vec{\xi})}\xi_1^{\ell_1}\xi_2^{\ell_2}\xi_3^{\ell_3}\,.$$

Obviously, μ_{0N} is non-negative whenever $\xi_1,\xi_2,\xi_3 \geq 0$ and hence defines a probability distribution. For $\xi_1=\xi_2=\xi$ and $\xi_3=0$ it is not difficult to see that this even holds true for $\xi \geq -\frac{1}{4}$, but not for $\xi_c \leq \xi < -\frac{1}{4}$. Similar remarks apply to μ_{iN} up to a sign factor. Our aim is to consider limits of the expectations $\langle\cdot\rangle_{iN}$ with respect to the (signed) distributions μ_{iN} as $N\to\infty$, for arbitrary values of $\vec{\xi}\in S$.

As a consequence of (6) and standard transfer theorems (see e.g. [20]) the following asymptotic behaviour of $W_{iN}(\vec{\xi})$ for large N holds:

$$W_{iN}(\vec{\xi}) = \Omega_i N^{-3/2} g_c(\vec{\xi})^{-N}(1+\mathrm{O}(\tfrac{1}{N})) \quad \text{if } \alpha = 1/2\,, \tag{22}$$
$$W_{iN}(\vec{\xi}) = \Omega_i N^{-4/3} g_c(\vec{\xi})^{-N}(1+\mathrm{O}(\tfrac{1}{N})) \quad \text{if } \alpha = 1/3\,, \tag{23}$$

where the constants Ω_i depend on $\vec{\xi}$. We note that the relations (3) imply

$$\Omega_1 = \xi_1\Omega_0 \tag{24}$$
$$\Omega_2 = \xi_2 W_{0c}\frac{2-\xi_2W_{0c}-g_c\xi_3W_{0c}}{(1-\xi_2W_{0c})^2(1-g_c\xi_3W_c)^2}\,\Omega_0\,. \tag{25}$$

Using (22) and (23) it follows by a straight-forward generalization of arguments given in [21, 18] that for any local quantity $A(\tau,\ell)$ depending only on the structure of (τ,ℓ) within a finite distance R from the root of τ, such as the volume of the ball $B_R(\tau)$ of radius R centered at the root, the limiting expectation values

$$\langle A\rangle_i = \lim_{N\to\infty}\langle A\rangle_{iN}$$

exist.

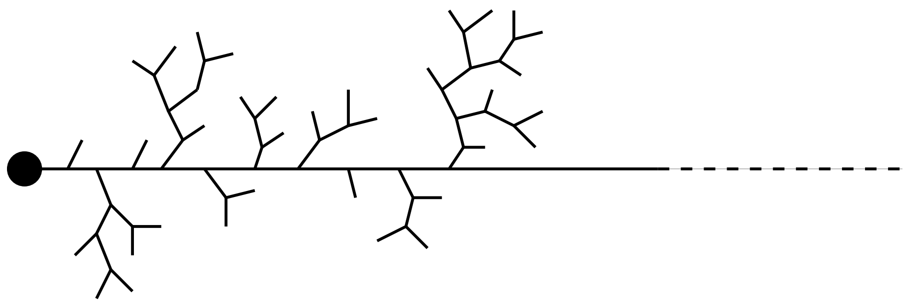

Figure 5: Finite trees attached to the first few vertices on the spine of an infinite tree.

We next briefly describe how to calculate the limiting expectation values $\langle A\rangle_i$ in terms of infinite labelled trees, further details can be found in [21, 18]. Here an infinite labelled tree means an infinite rooted planar tree with root of order 1 with a labelling respecting the same conditions a)- c) as previously. Moreover, only trees with a single spine, that is an infinite self-avoiding path starting at the root, contribute to $\langle A\rangle_i$, see Fig. 5. The spine vertices of an infinite labelled tree L will be denoted by $r, u_1, u_2, u_3, \ldots$, ordered by increasing distance from the root r. Thus L is obtained by grafting finite labelled trees with root of order 1, called branches, at the spine vertices u_i on both sides of the spine. Considering only the finite part $r, u_1, u_2, \ldots, u_N$ of the spine one of the branches rooted at u_N is infinite and all other branches are finite. We denote by $L(N)$ the finite labelled tree obtained by removing the infinite branch at u_N except the edge $u_N u_{N+1}$ and consider $L(N)$ as a finite labelled tree with a finite spine $r, u_1, u_2, \ldots, u_{N+1}$ both of whose end vertices have order 1. By $\mathcal{A}(L_0)$ we denote the set of all infinite labelled trees such that $L(N)$ equals a fixed finite labelled tree L_0 with a distinguished spine $r, u_1, u_2, \ldots, u_{N+1}$. With this notation the limiting weight of the set $\mathcal{A}(L_0)$ equals

$$\mu_i(\mathcal{A}(L_0)) = \Omega_i^{-1}\Omega_{\ell_{N+1}}\rho_i(L_0)\,, \tag{26}$$

where $\rho_i(L_0)$ is the grand canonical weight of $L_0 = (\tau_0, \ell_0)$ at the critical point $(\vec{\xi}; g_c)$ given by

$$\rho_i(\tau_0, \ell_0) = \delta_{\ell_0(u_1),i}\, g_c^{|\tau_0|-1}\xi_1^{\ell_{01}-\delta_{\ell_0(u_{N+1}),1}}\xi_2^{\ell_{02}-\delta_{\ell_0(u_{N+1}),2}}\xi_3^{\ell_{03}}\,. \tag{27}$$

The information contained in (26) and (27) suffices to calculate $\langle A\rangle_i$ for any local quantity A. We now proceed to calculate $\langle |B_R|\rangle_i$, where $|B_R(L)|$ denotes the size of $B_R(L)$, i.e. the number of edges in τ whose vertices are at graph distance at most R from the root. The *local Hausdorff dimension* d_h of the random tree defined by μ_i is defined by

$$\langle\, |B_R|\, \rangle_i \;\sim\; R^{d_h} \tag{28}$$

as $R \to \infty$. The purpose of the next two subsections is to evaluate d_h in the case $\xi_3 = 0$ and demonstrate that its value coincides with d_H as found in Section 3.

4.1 Volume of a finite tree for $\xi_1 = \xi_2 = \xi$, $\xi_3 = 0$

We let H_i^R denote the (unnormalized) expectation value of the number of vertices $h_R(\tau)$ at distance R from the root of a finite tree τ with label i on its vertex v_0 at the critical value $g_c(\xi)$ of the coupling g, that is

$$H_i^R = \sum_{(\tau;\ell):\ell(v_0)=i} h_R(\tau) g_c^{|\tau|} \xi^{\ell_1+\ell_2} \,. \tag{29}$$

Applying arguments similar to those leading to (3) one obtains, for $i = 0, 1, 2$,

$$\begin{aligned} H_i^1 &= W_{ic}\,, \\ H_i^R &= \sum_{j=0}^{2} \mathbb{T}(\xi, g_c(\xi))_{ij} H_j^{R-1}\,, \quad R \geq 2, \end{aligned} \tag{30}$$

where $\mathbb{T}$ is given by (14). $\mathbb{T}_c = \mathbb{T}(\xi, g_c(\xi))$ has eigenvalues

$$\lambda_0 = 0, \quad \lambda_1 = 1, \quad \lambda_2 = \frac{\xi^2 W_{0c}(\xi)^3}{g_c(\xi)}\,, \tag{31}$$

and right eigenvectors corresponding to the non-zero eigenvalues

$$\mathbf{e}^{(1)} = \mathbf{M} = \frac{W_{0c}^2}{g_c} \begin{pmatrix} 1 \\ \xi \\ g_c W_{0c}^{-2} - 1 - \xi \end{pmatrix}, \; \mathbf{e}^{(2)} = \frac{W_{0c}^2}{g_c} \begin{pmatrix} 1 \\ \xi \\ \lambda_2 g_c W_{0c}^{-2} - 1 - \xi \end{pmatrix}. \tag{32}$$

Here

$$\mathbf{M} = \Omega^{-1}(\Omega_0, \Omega_1, \Omega_2)\,,$$

where

$$\Omega = \sum_{i=0}^{2} \Omega_i\,,$$

such that $\sum_i M_i = 1$.

There are now two cases to consider:

<u>$\xi > \xi_c$</u> The eigenvalue $\lambda_2 < 1$, $\mathbb{T}_c$ is diagonalizable and it is straightforward to show that

$$\mathbf{H}^R = (1 - \lambda_2)^{-1} \left[(1 - (\lambda_2 + 1) g_c W_{0c}^{-1})\, \mathbf{M} + \lambda_2^{R-1} (2 g_c W_{0c}^{-1} - 1)\, \mathbf{e}^{(2)} \right]. \tag{33}$$

$\underline{\xi = \xi_c}$ The eigenvalue $\lambda_2 = 1$ and we see from (32) that its eigenvector coincides with $\mathbf{M}$ so $\mathbb{T}_c$ has non-trivial Jordan normal form and a new vector

$$\boldsymbol{\varepsilon} = \begin{pmatrix} 0 \\ 0 \\ 1 \end{pmatrix} \tag{34}$$

emerges satisfying

$$\mathbb{T}_c \, \boldsymbol{\varepsilon} = \mathbf{M} + \boldsymbol{\varepsilon}. \tag{35}$$

Setting

$$\mathbf{W} = (W_0, W_1, W_2)$$

and noting that

$$\mathbf{W}_c = g_c W_{0c}^{-1} \mathbf{M} + (1 - 2g_c W_{0c}^{-1}) \boldsymbol{\varepsilon} \tag{36}$$

then gives

$$\mathbf{H}^R = \mathbf{W}_c + (R-1)(1 - 2g_c W_{0c}^{-1}) \mathbf{M} \,, \quad R \geq 1 \,. \tag{37}$$

4.2 Volume of an infinite tree for $\xi_1 = \xi_2 = \xi$, $\xi_3 = 0$

We let K_i^R denote the (unnormalized) expectation value with respect to the measure μ_i of the number $k_R(\tau)$ of vertices at distance R from the root of an infinite tree τ up to a normalization factor. Specifically,

$$K_i^R = \Omega^{-1} \, \Omega_i \, \langle k_R \rangle_i \,.$$

By decomposing the tree into its branches at the vertex u_1 next to the root one finds that K_i^R satisfies

$$K_i^R = \frac{\partial F_i}{\partial W_j} K_j^{R-1} + M_j \frac{\partial^2 F_i}{\partial W_j \partial W_k} H_k^{R-1} \tag{38}$$

or

$$\mathbf{K}^R = \mathbb{T}_c \mathbf{K}^{R-1} + \Gamma \mathbf{H}^{R-1} \tag{39}$$

where

$$\Gamma_{ik} = M_j \frac{\partial^2 F_i}{\partial W_j \partial W_k} = M_j \Lambda_{i,jk}. \tag{40}$$

The first term in (39) is the contribution of the infinite branch and the second term that of the finite branches. As each tree has only a single vertex at height 1,

$$\mathbf{K}^1 = \mathbf{M}. \tag{41}$$

The equation (39) is easily iterated to get

$$\mathbf{K}^R = \mathbf{M} + \sum_{\ell=1}^{R-1} \mathbb{T}_c^{\ell-1} \, \Gamma \, \mathbf{H}^{R-\ell}. \tag{42}$$

There are again two cases to consider:

$\underline{\xi > \xi_c}$ Combining (33) and (42) and noting that

$$\Gamma \, \mathbf{M} = 2 g_c^{-1} W_{0c} \, \mathbf{M} \tag{43}$$

gives

$$\mathbf{K}^R = 2 \, \frac{(W_{0c} g_c^{-1} - \lambda_2 - 1)}{1 - \lambda_2} \, R \, \mathbf{M} + O(1) \tag{44}$$

from which we get

$$\langle |B_R| \rangle_i = \Omega_i^{-1} \, \Omega \sum_{n=1}^{R} K_i^n = \Omega \, \frac{(W_{0c} g_c^{-1} - \lambda_2 - 1)}{1 - \lambda_2} \, R^2 + O(R). \tag{45}$$

It is straightforward to check that the coefficient of the R^2 term is positive for all $\xi > \xi_c$ so we have shown that $d_h = 2$ in this regime. Note also that the coefficient diverges at $\xi = \xi_c$, where $\lambda_2 \to 1$, indicating that d_h changes there.

$\underline{\xi = \xi_c}$ Combining (37) and (42) we have

$$\begin{aligned} \mathbf{K}^R = \mathbf{M} \; &+ \; \sum_{\ell=1}^{R-1} \mathbb{T}_c^{\ell-1} \, \Gamma \left((1 - 2 g_c W_{0c}^{-1})(\boldsymbol{\varepsilon} - \mathbf{M}) + g_c W_{0c}^{-1} \mathbf{M} \right) \\ &+ \; \sum_{\ell=1}^{R-1} \mathbb{T}_c^{\ell-1} \, \Gamma \left((R - \ell)(1 - 2 g_c W_{0c}^{-1}) \mathbf{M} \right) \end{aligned} \tag{46}$$

It is straightforward to check that at the tricritical point

$$\Gamma \, \boldsymbol{\varepsilon} = 2 g_c^{-1} W_{0c} \left(\mathbf{M} + \frac{1}{2} \boldsymbol{\varepsilon} \right). \tag{47}$$

Using this identity and (35) then gives

$$\mathbf{K}^R = 3 \left(\frac{W_{0c}}{2 g_c} - 1 \right) R^2 \, \mathbf{M} + O(R). \tag{48}$$

It is worth noting that one might have supposed from (35), (37) and (42) that $\mathbf{K}^R$ would be $O(R^3)$; however the coefficient of this leading term vanishes as a consequence of the tri-criticality condition. It follows now that

$$\langle|B_R|\rangle_i = \Omega_i^{-1}\,\Omega \sum_{n=1}^{R} K_i^n = \Omega\left(\frac{W_{0c}}{2g_c}-1\right)R^3 + O(R^2) \tag{49}$$

The coefficient of the R^3 term evaluates to a positive number so we have shown that $d_h = 3$ at $\xi = \xi_c$ in the AZ model.

5 The extended model $\xi_3 \neq 0$

In [16] it was argued that the AZ model with the CDT coupled to a reduced set of dimers is not likely to differ significantly from the full CDT-with-dimers system (hereafter called CDT-D). We claim here that this is probably not correct by considering what happens when $\xi_3 \neq 0$; this perturbation is arguably closer to the CDT-D model as it incorporates more of the possible dimer types than the AZ model.

In the most general case $\mathbb{T}$ is given by

$$\mathbb{T}(\xi;g) = H\begin{pmatrix} g(1+g\xi_3W_1)H & W_0 & W_0(1-g\xi_3W_0) \\ g\xi_1(1+g\xi_3W_1)H & W_1 & W_1(1-g\xi_3W_0) \\ g\xi_2(1-W_1(1-g\xi_3W_2))H & W_2 & \xi_2W_0(1-W_1-g\xi_3W_0) \end{pmatrix}. \tag{50}$$

It is straightforward although tedious to show that on the critical surface $g_c(\xi_1,\xi_2,\xi_3)$

$$\mathbf{M} = \frac{W_{0c}^2}{g_c}\left(1+\xi_3(1+\xi_1)W_0^3(2-g\xi_3W_0)\right)^{-1}\begin{pmatrix} 1 \\ \xi_1 \\ g_cW_{0c}^{-2}-(1+\xi_1)(1-g\xi_3W_0)^2 \end{pmatrix} \tag{51}$$

is always a right eigenvector with eigenvalue 1 and that the other eigenvalues are 0 (corresponding to the fact that $F_1 = \xi_1F_0$) and

$$\lambda_2 = \frac{\xi_1\xi_2W_0^3}{g(1-g\xi_3W_0)^2} = g\xi_1\xi_2W_0H^2\,, \tag{52}$$

where we have used

$$H = \frac{W_0}{g(1-g\xi_3W_0)}\,.$$

For definiteness we will first discuss the model with $\xi_1 = \xi_2 = \xi_3 = \xi$ which, at least naively, is the closest we can get to CDT-D. For $\xi > \xi_c \approx -0.228$ we find that g_c is a square root singularity of W_0, so $\alpha = \frac{1}{2}$, and $\lambda_2 < 1$ at $g = g_c$.

Consequently $m(g) \sim |\Delta g|^{\frac{1}{2}}$ and $d_H = 2$ following the discussion of Section 3. The infinite graph calculation of the local Hausdorff dimension follows the same lines as the $\xi > \xi_c$ case in Section 4 leading to $d_h = 2$. In this region of parameter space, where the dimer system is not critical, the model has exactly the same properties as the AZ model.

However at $\xi = \xi_c$ there is a tricritical point at which $\mathbb{T}_c$ is diagonalisable, $\lambda_2 \approx 0.445 < 1$ and $m(g) \sim |\Delta g|^{\frac{2}{3}}$ (the absence of a $|\Delta g|^{\frac{1}{3}}$ term is a consequence of the tricriticality condition). Thus $d_H = \frac{3}{2}$ but, as shown in the Appendix, $d_h = 1$. It is interesting to compare this result with the simpler multicritical tree model of rooted binary trees with dimers placed on the edges, including the root edge, in such a way that no more than one dimer can end at any vertex [17]. Letting W_1 and W_0 be the partition functions for trees with and without a dimer on the root edge respectively we see that they satisfy equations of the same form as (3) but with

$$\begin{aligned} F_0 &= g(W_0^2 + 2W_0W_1 + 1) \\ F_1 &= g\xi(W_0^2 + 1). \end{aligned} \tag{53}$$

This model also has a tricritical point with $\xi_c = -\frac{4}{27}$, exponent $\alpha = \frac{1}{3}$ and $\lambda_{2c} < 1$. One finds that

$$\Delta\lambda_1 \sim \frac{\partial g}{\partial W_0} \sim (\Delta W_0)^2 \sim |\Delta g|^{2/3}. \tag{54}$$

which implies that $d_H = 3/2$ for $\xi = \xi_c$. On the other hand, using the results of the Appendix, $d_h = 1$ as there is once again only one unit eigenvalue of $\mathbb{T}_c$. The $\xi_1 = \xi_2 = \xi_3$ line of our model thus exhibits exactly the same behaviour as a standard multi-critical tree model.

These calculations appear to show that the degenerate tri-critical point with $d_h = 3$ found in the AZ model is very special and not at all characteristic of CDT dimer models in general. It is instructive to examine the phase diagram in the $(\xi_1 = \xi_2 = \xi, \xi_3)$ plane, see Fig 6. There is a line of cubic degeneracies in W_0 that takes in the point $(-0.278\ldots, 0)$ and extends both above and below the ξ axis. Using (52) and the identity

$$g^2\xi^2H^3 - g^2(1+\xi)\xi_3H^3 - 1 = 0$$

which holds at tricritical points as a consequence of (8),(9) and (10) it follows that

$$\lambda_2 = 1 + g_c\xi_3(1 + \xi - \xi^2W_0)H^3\,.$$

Since the expression in parenthesis, H and g_c are all positive it follows that on the tricritical line $\lambda_2 < 1$ for $\xi_3 < 0$ but that $\lambda_2 > 1$ for $\xi_3 > 0$. The latter behaviour is a little strange; it would in fact be a contradiction for a purely real eigenvalue

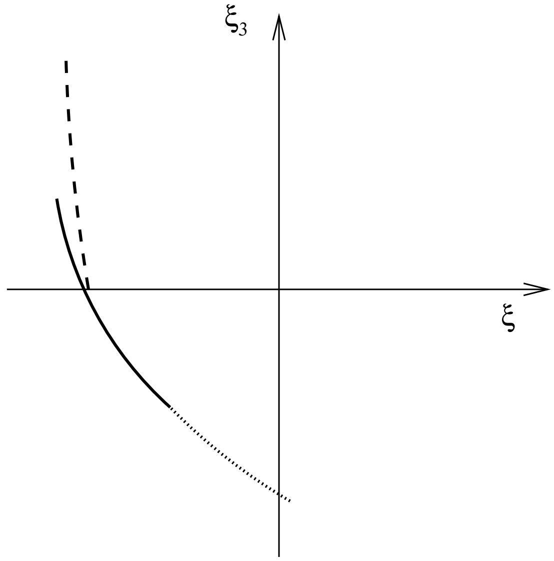

Figure 6: The phase diagram in the ($\xi_1 = \xi_2 = \xi$, ξ_3) plane. The solid line is the line of cubic degeneracies in W_0. For $\xi_3 > 0$ the physical region S defined in Sec. 2 lies to the right of the long dashed line, which is the line where $\lambda_2 = 1$. For $\xi_3 \leq 0$ the first part of the boundary of S is the lower part of the solid line of cubic degeneracies in W_0. The dotted line makes up the rest of the lower part of the boundary of S. Along this part W_0 is only quadratic degenerate.

of $\mathbb{T}$ to go through 1 *before* criticality is reached (see the Appendix for example). Closer inspection shows that at small $g \ll g_c$ the eigenvalues are complex and as g increases they flow as shown in Fig 7. However exponential growth of the two-point function is a symptom that the series in ξ_i and $g < g_c$ for Z is not absolutely convergent and the effect of the negative weights is sufficiently strong that the conventional statistical mechanical interpretation of the model fails. We conclude that the physical region for $\xi_3 > 0$ extends only as far as the line where $\lambda_2 = 1$ at g_c. It can be checked that inside the region and along this line there are only quadratic degeneracies in W_0 and that $\mathbb{T}_c$ is diagonalisable so $d_h = d_H = 2$. On the other hand for $\xi_3 < 0$ there is a genuine line of tricriticality which includes the $\xi = \xi_3$ point analysed above and ends at $(-0.162\ldots, -0.582\ldots)$. Beyond this point the tricriticality disappears and even on the boundary of the physical region $\alpha = \frac{1}{2}$ and $d_h = d_H = 2$.

6 Concluding remarks

At the critical value of the dimer fugacity we expect that CDT-D, the full dimer model on CDT, represents a lattice regularization of projectable Hořava-Lifshitz

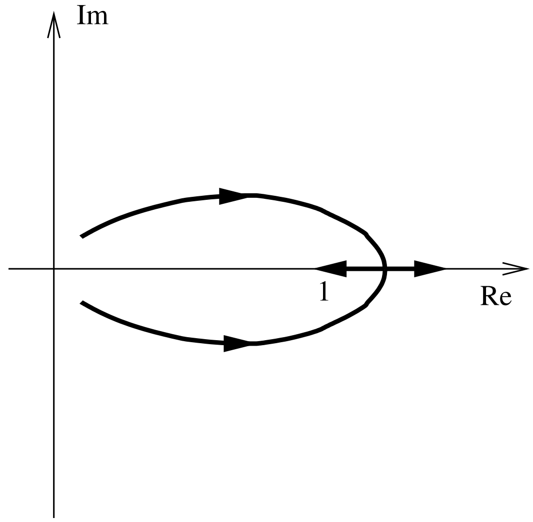

Figure 7: The flow in the complex plane of the non-zero eigenvalues of $\mathbb{T}$; the arrow heads show how they move as g increases; λ_1 ends at 1, λ_2 at a value > 1.

quantum gravity coupled to a (2,5) minimal conformal field theory. In the absence of a solution to CDT-D we have obtained the solution of a restricted dimer model and mapped out its phase diagram. In particular, we have seen that the geometric features of the AZ model [16] are very special and not robust under perturbations. At generic points of the phase boundary we have found the values of the Hausdorff dimensions are either $d_H = 3/2$ and $d_h = 1$, coinciding with the values for the simplest multicritical tree [23, 19], or $d_H = d_h = 2$.

One may speculate on the implications of our results for the CDT-D model. While we do not have any rigorous results in this direction it is worth noting that the full dimer model on a generalized CDT [24] has been solved exactly in [17] using a matrix model representation yielding the value $d_H = 3/2$. The generalized causal triangulations of this model can be defined combinatorially [25] or by using a special scaling limit of matrix models [24]. This slightly more general set of triangulations has many of the characteristics of CDT, e.g. $d_H = d_h = 2$. Hence it is tempting on the basis of this result to conjecture that $d_H = 3/2$ and $d_h = 1$ are indeed the correct values for the full dimer model on a CDT.

It is natural to extend the above considerations further. One can define multicritical generalized CDT models [26], which most likely correspond to specific fine-tuned scaling limits of matrix models, generalizing the considerations in [17]. Recall that the standard multicritical matrix models from DT provide representations of 2d Euclidean quantum gravity coupled to certain conformal field theories. They also have the interpretation of (increasingly complicated) fine-tuned multi-dimers systems on the DT-set of random graphs. Thus it is possible that the multicritical behavior found in [26] represents the effect of fine-tuned multi-dimer models on the generalized CDT-set of random graphs, and has the continuum interpretation of certain conformal field theories coupled to 2d Hořava-Lifshitz gravity.

This leave us with the interpretation of the AZ model. Although this model is special, it is not *that* special. As we have seen there is a least a one-parameter set of coupling constants leading to the same scaling. Thus we believe there should also be a continuum interpretation of this class of models.

Acknowledgements.

J.A. acknowledges support from the ERC Advanced Grant 291092 "Exploring the Quantum Universe" (EQU) as well as from the Free Danish Research Council grant "Quantum gravity and the role of black holes." In addition JA was supported in part by the Perimeter Institute of Theoretical Physics. Research at Perimeter Institute is supported by the Government of Canada through Industry Canada and by the Province of Ontario through the Ministry of Economic Development & Innovation. J.A. and B.D. acknowledge support from NordForsk researcher network Random Geometry (grant no. 33000)".

Appendix: d_h and the multi-critical condition

We discuss here how the condition for multi-criticality affects d_h in general. We consider a set of generalised trees with first vertex label $\ell(v_0) = i$ whose partition functions W_i satisfy

$$W_i = F_i(\mathbf{W}; \vec{\xi}; g), \qquad i = 1 \dots N. \tag{55}$$

The approach to criticality in the grand canonical ensemble (GCE) is governed by (repeated indices are summed over)

$$\delta W_i = \delta g \frac{\partial F_i}{\partial g} + \mathbb{T}_{ij} \delta W_j + \frac{1}{2} \Lambda_{i,jk}\, \delta W_j \delta W_k + \text{h.o.t.} \tag{56}$$

where

$$\mathbb{T}_{ij} = \frac{\partial F_i}{\partial W_j}, \quad \Lambda_{i,jk} = \frac{\partial^2 F_i}{\partial W_j \partial W_k}, \quad (\mathbf{\Lambda}_{jk})_i = \Lambda_{i,jk}. \tag{57}$$

Re-arranging

$$((1 - \mathbb{T})\delta W)_i = W_i \delta g + \frac{1}{2} \Lambda_{i,jk}\, \delta W_j \delta W_k + \text{h.o.t.} \tag{58}$$

so criticality is reached as $g \uparrow g_c$ where the largest real eigenvalue of $\mathbb{T}$ first reaches 1.

Now, setting $g = g_c$ and working in the critical ensemble, consider the infinite single spine trees with first vertex labelled by $\ell(u_1) = i$. Decomposing these trees at their first vertex u_1 into an infinite component and finite components we see that their measures M_i satisfy

$$M_i = \left(\frac{\partial F_i}{\partial W_j}\right)_c M_j = \mathbb{T}_{cij} M_j. \tag{59}$$

We will assume that they are normalised so that the total measure is 1,

$$1 = \sum_i M_i. \tag{60}$$

We see that $\mathbb{T}$ directly relates the infinite spine trees and the GCE. At criticality it must have at least one eigenvalue which is one and this must be the first real eigenvalue to reach one, otherwise the system would have reached criticality at some smaller value of g.

Turning to the local Hausdorff dimension we note from (42), (30) and (59) that K_i^R, the expectation value with respect to the measure μ_i of the number of vertices at distance R from the root of an infinite tree, is given by

$$\mathbf{K}^R \quad = \quad \mathbf{M} + \sum_{\ell=1}^{R-1} \mathbb{T}^{\ell-1}\, \Gamma\, \mathbb{T}^{R-\ell-1}\, \mathbf{W}, \tag{61}$$

where

$$\Gamma_{ik} = M_j \frac{\partial}{\partial W_k}\left(\frac{\partial F_i}{\partial W_j}\right) = M_j \Lambda_{i,jk}. \tag{62}$$

The implications in general of (61) for the Hausdorff dimension depend very much upon the Jordan decomposition of $\mathbb{T} = SJS^{-1}$ where J is of Jordan Block form $\mathrm{Diag}(J^<, J^1)$; the block J^1 corresponds to r unit eigenvalues and $J^<$ to the $N - r$ eigenvalues which are less than 1. If J^1 is diagonal then

$$J^\ell = \mathrm{Diag}(0, \ldots 0, 1, \ldots 1) + O(\alpha^\ell) \tag{63}$$

where α is the largest eigenvalue smaller than 1.

We first consider the case where there is a single unit eigenvalue so $J^1 = 1$. Introduce the orthonormal basis $(\mathrm{e}^i)_j = \delta_{ij}$ so that

$$\delta\mathbf{W} \quad = \quad S(\mu\, \mathrm{e}^N + \nu^a\, \mathrm{e}^a)\,, \qquad \mathbf{W} = S(A\, \mathrm{e}^N + B^a\, \mathrm{e}^a) \tag{64}$$

where $a, b = 1 \ldots N-1$. $A \neq 0$ and B^a are constants and up to normalisation the measure vector is

$$\mathbf{M} = S\, \mathrm{e}^N. \tag{65}$$

Substituting in (58) we obtain

$$
\begin{aligned}
(1-J^{<})\nu^a\,\mathrm{e}^a &= (A\,\mathrm{e}^N + B^a\,\mathrm{e}^a)\delta g + \frac{1}{2}\mu^2 S^{-1}\Gamma S\mathrm{e}^N + \mu\nu^a S^{-1}\Gamma S\,\mathrm{e}^a \\
&\quad + \frac{1}{2}\nu^a\nu^b S^{-1}\mathbf{\Lambda}_{jk}(S\,\mathrm{e}^a)_j(S\,\mathrm{e}^b)_k\,. \qquad (66)
\end{aligned}
$$

Since $1-J^{<}$ is invertible we see that, provided $(S^{-1}\Gamma S)_{NN}$ is non-zero, $\mu\sim(\delta g)^{\frac{1}{2}}$ and criticality is quadratic. The multi-critical condition is

$$
(S^{-1}\Gamma S)_{NN}=0. \qquad (67)
$$

Now returning to (61)

$$
\mathbf{K}^R = \mathbf{M} + \sum_{\ell=1}^{R-1} SJ^{\ell-1}\,S^{-1}\Gamma\,SJ^{R-\ell-1}S^{-1}\,\mathbf{W} \qquad (68)
$$

whence, using (63),

$$
\mathbf{K}^R = \mathbf{M} + R\,\mathbf{S}\,(S^{-1}\Gamma\,S)_{NN}(S^{-1}\,\mathbf{W})_N + O(1) \qquad (69)
$$

where $\mathbf{S}_i = S_{iN}$. We see from (67) and (69) that the linear term linear in R automatically vanishes at the multi-critical point where, therefore, $d_h=1$. This is completely standard multi-criticality and the result is identical to that for the single component multi-critical tree. It is straightforward to generalise this analysis to models where J^1 is of higher rank but still diagonal and find the same conclusion that $d_h=1$. Note that it is always necessary to compute the actual coefficient of the remaining leading term in a particular model to check that it is positive otherwise the result is meaningless.

The situation is different if J^1 is non-diagonal. We will analyse the simplest case where there are two unit eigenvalues and we have the simplest non-diagonal Jordan block

$$
J^1 = \begin{pmatrix} 1 & 1 \\ 0 & 1 \end{pmatrix}. \qquad (70)
$$

We then have that

$$
(J^\ell)_{ij} = \delta_{i,N-1}\delta_{j,N-1} + \delta_{i,N}\delta_{j,N} + \ell\delta_{i,N-1}\delta_{j,N} + O(\alpha^\ell). \qquad (71)
$$

$\mathbf{M}$ is the ordinary eigenvector with eigenvalue 1,

$$
\mathbf{M} = S\mathrm{e}^{N-1} \qquad (72)
$$

but now there is a vector belonging to the second eigenvalue 1

$$\boldsymbol{\varepsilon} = S\mathrm{e}^N \tag{73}$$

with the property

$$\mathbb{T}\,\boldsymbol{\varepsilon} = \mathbf{M} + \boldsymbol{\varepsilon}. \tag{74}$$

Now we have

$$\delta\mathbf{W} \;=\; S(\mu\,\mathrm{e}^{N-1} + \lambda\,\mathrm{e}^N + \nu^a\,\mathrm{e}^a)\,, \quad \mathbf{W} = S(A\,\mathrm{e}^N + C\,\mathrm{e}^{N-1} + B^a\,\mathrm{e}^a)\,, \tag{75}$$

where $a, b = 1 \dots N-2$. $A \neq 0$ and B^a are constants and substituting in (58) we find

$$\begin{aligned}(1-J^{<})\nu^a\,\mathrm{e}^a + \lambda\,\mathrm{e}^{N-1} \;&=\; (A\,\mathrm{e}^N + C\,\mathrm{e}^{N-1} + B^a\,\mathrm{e}^a)\delta g + \\ &+\frac{1}{2}S^{-1}\boldsymbol{\Lambda}_{jk}\,(\mu\,\mathbf{M} + S\lambda\,\mathrm{e}^N + \nu^a S\,\mathrm{e}^a)_j \times \\ &S(\mu\,\mathrm{e}^{N-1} + \lambda\,\mathrm{e}^N\mu\,\mathbf{M} + \nu^b\mathrm{e}^b)_k + \text{h.o.t.}\end{aligned} \tag{76}$$

and closing with e^N,

$$0 \;=\; A\delta g + \frac{1}{2}\mu^2(S^{-1}\Gamma S)_{NN-1} + \dots \tag{77}$$

showing that

$$(S^{-1}\Gamma S)_{NN-1} = 0 \tag{78}$$

is a necessary condition for multi-criticality. Note that because of the Jordan block structure λ appears linearly on the l.h.s. of (76) so the leading singularity can only be associated with $\mathbf{M}$, and not with $\boldsymbol{\varepsilon}$. Using (61) and (71) we get

$$\begin{aligned}\mathbf{K}_i^R \;&=\; \mathbf{M}_i + \sum_{\ell=1}^{R-1} S_{ij'}(\delta_{j',N-1}\delta_{j,N-1} + \delta_{j',N}\delta_{j,N} + (\ell-1)\delta_{j',N-1}\delta_{j,N}) \\ &\quad (S^{-1}\Gamma\,S)_{jn}(\delta_{n,N-1}\delta_{m,N-1} + \delta_{n,N}\delta_{m,N} + (R-\ell-1)\delta_{n,N-1}\delta_{m,N})(S^{-1}\,\mathbf{W})_m + O(1) \\ &=\; \mathbf{M}_i + \frac{1}{6}(R-1)(R-2)(R-3)S_{iN-1}(S^{-1}\Gamma\,S)_{NN-1}(S^{-1}\,\mathbf{W})_N \\ &\quad +\frac{1}{2}(R-1)(R-2)\sum_{L=N-1}^{N}\left[S_{iN-1}(S^{-1}\Gamma\,S)_{NL}(S^{-1}\,\mathbf{W})_L + \,S_{iL}(S^{-1}\Gamma\,S)_{LN-1}(S^{-1}\,\mathbf{W})_N\right] \\ &\quad +O(R)\end{aligned} \tag{79}$$

We see from (79) that the multi-critical condition automatically suppresses the $(R-1)(R-2)(R-3)$ in $\mathbf{K}^R$ but that the quadratic $(R-1)(R-2)$ term survives. Hence $d_h = 3$, again provided that the numerical coefficient, which has to be computed in a particular model, is positive.

References

[1] B. Durhuus, J. Frohlich and T. Jonsson, Nucl. Phys. B **240** (1984) 453; Phys. Lett. B **137** (1984) 93.

[2] F. David, Nucl. Phys. **B257** (1985) 45.
A. Billoire and F. David, Phys. Lett. B **168** (1986) 279-283.
J. Ambjorn, B. Durhuus and J. Fröhlich, Nucl. Phys. B **257** (1985) 433-449;
J. Ambjorn, B. Durhuus, J. Fröhlich and P. Orland, Nucl. Phys. B **270** (1986) 457-482.
V. A. Kazakov, A. A. Migdal, I. K. Kostov, Phys. Lett. **B157** (1985) 295-300.
D.V. Boulatov, V.A. Kazakov, I.K. Kostov and A.A. Migdal, Nucl. Phys. B **275** (1986) 641-686.

[3] J. Ambjørn and J. Jurkiewicz, Phys. Lett. B **278** (1992) 42-50.
M.E. Agishtein and A.A. Migdal, Mod. Phys. Lett. A **7** (1992) 1039-1062.

[4] P. Bialas, Z. Burda, A. Krzywicki, B. Petersson: Nucl. Phys. B472 (1996) 293-308. [hep-lat/9601024].
B.V. de Bakker: Phys. Lett. B 389 (1996) 238-242 [hep-lat/9603024].
S. Catterall, R. Renken, J. B. Kogut: Phys. Lett. B416 (1998) 274-280. [hep-lat/9709007].

[5] J. Ambjorn, R. Loll, Nucl. Phys. B 536 (1998) 407-434 [hep-th/9805108].

[6] J. Ambjorn, J. Jurkiewicz and R. Loll: Phys. Rev. Lett. **85** (2000) 924, [hep-th/0002050].

[7] P. Hořava, Phys. Rev. D **79** (2009) 084008 [arXiv:0901.3775, hep-th].
P. Hořava and C.M. Melby-Thompson, Phys. Rev. D **82** (2010) 064027 [arXiv:1007.2410, hep-th].

[8] J. Ambjorn, A. Goerlich, J. Jurkiewicz and R. Loll, *Nonperturbative Quantum Gravity,* Phys. Rept. **519** (2012) 127 [arXiv:1203.3591 [hep-th]].

[9] P. Di Francesco, E. Guitter and C. Kristjansen, Nucl. Phys. B **567** (2000) 515 [hep-th/9907084].

[10] J. Ambjorn, L. Glaser, Y. Sato and Y. Watabiki, Phys. Lett. B **722** (2013) 172 [arXiv:1302.6359 [hep-th]].

[11] J. Ambjorn and A. Ipsen, Phys. Rev. D **88** (2013) 6, 067502 [arXiv:1305.3148 [hep-th]].

[12] J. Ambjorn, K. N. Anagnostopoulos and R. Loll, Phys. Rev. D **60** (1999) 104035 [hep-th/9904012].

[13] J. Ambjorn, K. N. Anagnostopoulos, R. Loll and I. Pushkina, Nucl. Phys. B **807** (2009) 251 [arXiv:0806.3506 [hep-lat]].

[14] J. Ambjorn, K. N. Anagnostopoulos and R. Loll, Phys. Rev. D **61** (2000) 044010 [hep-lat/9909129].

[15] J. Ambjorn, A. T. Goerlich, J. Jurkiewicz and H. -G. Zhang, Nucl. Phys. B **863** (2012) 421 [arXiv:1201.1590 [gr-qc]].

[16] M. R. Atkin, S. Zohren An Analytical Analysis of CDT Coupled to Dimer-like Matter. Phys. Lett. B **712** (2012) 445-450

[17] J. Ambjorn, L. Glaser, A. Gorlich and Y. Sato, Phys. Lett. B **712** (2012) 109 [arXiv:1202.4435 [hep-th]].

[18] B. Durhuus, T. Jonsson and J. Wheater, On the Spectral Dimension of Causal Trangulations. J. Stat. Phys. **139** (2010) 859-881

[19] J. Ambjorn, B. Durhuus and T. Jonsson, *Quantum geometry. A statistical field theory approach.* Cambridge University Press, Cambridge, 1997.

[20] P. Flajolet and R. Sedgewick, *Analytic Combinatorics.* Cambridge University Press, Cambridge, 2009.

[21] B. Durhuus, Probabilistic aspects of infinite trees and surfaces. Acta. Phys. Pol. **34** (2003) 4795-4811

[22] M. Staudacher, Nucl. Phys. B **336** (1990) 349.

[23] J. Ambjorn, B. Durhuus and T. Jonsson, Phys. Lett. B **244** (1990) 403.

[24] J. Ambjorn, R. Loll, W. Westra and S. Zohren, JHEP **0712** (2007) 017 [arXiv:0709.2784, gr-qc];
Phys. Lett. B **665** (2008) 252-256 [arXiv:0804.0252, hep-th];
Phys. Lett. B **670** (2008) 224 [arXiv:0810.2408, hep-th].
JHEP **0805** (2008) 032 [arXiv:0802.0719, hep-th].

[25] J. Ambjorn and T. G. Budd, J. Phys. A: Math. Theor. **46** (2013) 315201 [arXiv:1302.1763 [hep-th]].

[26] M. R. Atkin and S. Zohren, JHEP **1211** (2012) 037 [arXiv:1203.5034 [hep-th]].